

CHAPTER 19

Eight Years Wave Hindcast and Analysis of Wave Climate

Yoshio Hatada¹ and Masataka Yamaguchi²

Abstract

This paper deals with 8 years of wave hindcast at 11 wave observation points along the coast of the Japan Sea using a long-term shallow water wave hindcast system, and investigation of its applicability to the estimation of wave climate. Comparison with observations for not only time variations of significant waves but also long-term sea state indices such as yearly-averaged wave height and period. The availability of the present system and the advantages over the deep water wave hindcast system previously developed by the authors are verified by close and more reasonable agreement with the observed data including mean wave direction.

1. Introduction

Quantitative estimation of long term wave conditions over several years, so-called wave climate is a subject of great importance for the mitigation of wave-caused disaster and efficient utilization of wave energy. Up to now, the analysis of wave climate has relied on the observed wave data or wave data hindcasted with a simple wave prediction model such as the SMB method. In the former case, data of wave direction which are crucial to analysis of shore processes have seldom been observed and wave gauges have often broken down during severe wave conditions. In the latter case, conventional methods do not always give a satisfactory accuracy for hindcasted

-
- 1 Research Assistant, Dept. of Civil and Ocean Eng., Ehime Univ., Bunkyocho 3, Matsuyama 790, Ehime Pref., Japan
 - 2 Prof., Dept. of Civil and Ocean Eng., Ehime Univ., Bunkyocho 3, Matsuyama 790, Ehime Pref., Japan

waves and tremendous efforts are needed for hindcasting long term wave conditions.

Yamaguchi et al.(1990) developed a long term wave hindcast system which makes it possible to consecutively follow wave conditions over several years with reasonable accuracy. The system was applied to compute wave characteristics over 2 years every hour at 14 selected points along the coast of the Japan Sea. Close agreement between computation and observation for time variations of significant waves and wave direction as well as long term wave statistics verified the validity of the system. But the hindcast period of 2 years is too short to properly evaluate the wave climate when variability of the sea states is taken into account, and the wave model used is a deep water model with an approximate correction for shallow water effect.

The aim of this paper is to re-examine the applicability of a newly-revised system based on the comparison between computation and observation over 8 years at 11 wave observation points along the coast of the Japan Sea.

2. Outline of Long-Term Wave Hindcast System

(1) Wind hindcast model

The system consists of a wind estimation model and a wave estimation model. The wind model produces time variations of wind distribution over sea by spatial interpolation onto a regular grid of atmospheric pressure observed at irregularly-distributed points surrounding the sea area and the application of the wind model proposed by Bijvoet(1957). Either of -1°C or 0°C or 1°C every year on the entire region was given for data of air-water temperature difference which determines coefficients in the Bijvoet wind model, so that hindcasted results agree with observed results to the best possible degree, because it is hard to acquire long-term data of air and water temperatures.

Fig. 1 is a grid system divided into 28 by 41 with a grid distance of 80 km for the computation of atmospheric pressure and wind distributions over the Japan Sea, which includes 43 pressure observation points with the WMO location number. Surface atmospheric pressure data at the observation points and central positions of lows or highs over 8 years ranging from 1982 to 1989 every 3 hours are acquired from the magnetic tapes of meteorological data prepared by the Japan Meteorological Agency and direct inspection of the weather charts. Extraordinary values of observed pressure data are corrected by checking time series of the data and inspecting the corresponding

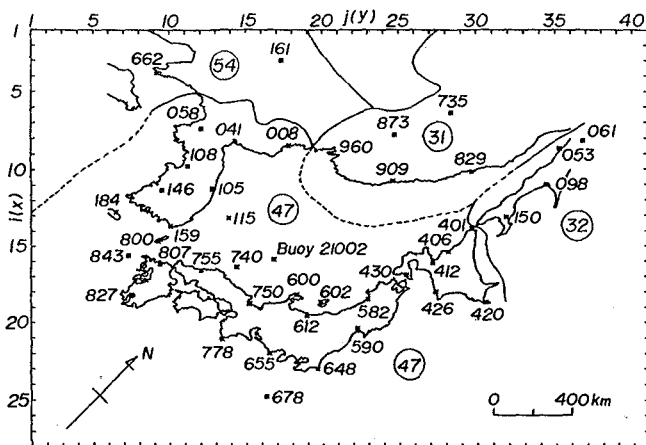


Fig. 1 Grid for computing wind distribution, and input points of observed atmospheric pressure.

weather charts. Before the wind computation, the pressure data interpolated on grids are smoothed three times, making use of a weighted smoothing formula with data of the surrounding 9 grid points in order to avoid overestimation of wind speed.

(2) Wave hindcast model

Wave estimation is due to a shallow water wave model (Yamaguchi et al., 1987) which belongs to a decoupled propagation model, tracing the change of directional spectrum along a refracted ray of each component focused on a hindcast point. The basic equation in the model is the radiative transfer equation in shallow water and is given by

$$\frac{\partial F}{\partial t} + c_g \cos \theta \frac{\partial F}{\partial x} + c_g \sin \theta \frac{\partial F}{\partial y} + \frac{c_g}{c} \left(\sin \theta \frac{\partial c}{\partial x} - \cos \theta \frac{\partial c}{\partial y} \right) \frac{\partial F}{\partial \theta} = c c_g S(f, \theta) \quad (1)$$

where $F = c c_g E(f, \theta)$, c is the celerity of a wave component, c_g the group velocity of a wave component, $E(f, \theta)$ the directional spectrum, f the frequency, θ the direction and $S(f, \theta)$ the source function. Source function consists of linear growth term by the Phillips mechanism, exponential growth term by the Miles mechanism and energy dissipation terms by pseudo-viscosity, bottom friction and opposing winds. Energy dissipation due to wave breaking is evaluated by imposing the condition that directional spectrum at growth stage can not exceed beyond an equilibrium directional spectrum in shallow water. This equilibrium spectrum is given by the product of the Pierson-Moskowitz spectrum with the correction term proposed by Thornton (1977) for shallow water effect and $\cos^4 \theta$

angular spreading function.

Eq. (1) is solved by a fractional time step method which computes propagation equation, and growth or decay equation alternately in each time step. At the first step, the propagation equation setting the right hand side of Eq. (1) to zero is solved by a full ray method or a piecewise ray method, which is a kind of the characteristic method. Full ray method is used for the computation of low frequency components satisfying the condition of $kh < 4$ at a hindcast point which can be regarded as shallow water waves, where h is the water depth at a hindcast point and k the wave number of the corresponding component, and piecewise ray method is used for the computation of high frequency components with $kh > 4$ which can be regarded as deep water waves. At the second step, the computation of growth or decay equation, which sets the propagation term in Eq. (1) to zero is conducted with the analytical solution using the results of propagation step as an initial value. When the directional spectrum computed at growth stage exceeds the shallow water equilibrium spectrum, it is reduced so as to get equal to the equilibrium spectrum.

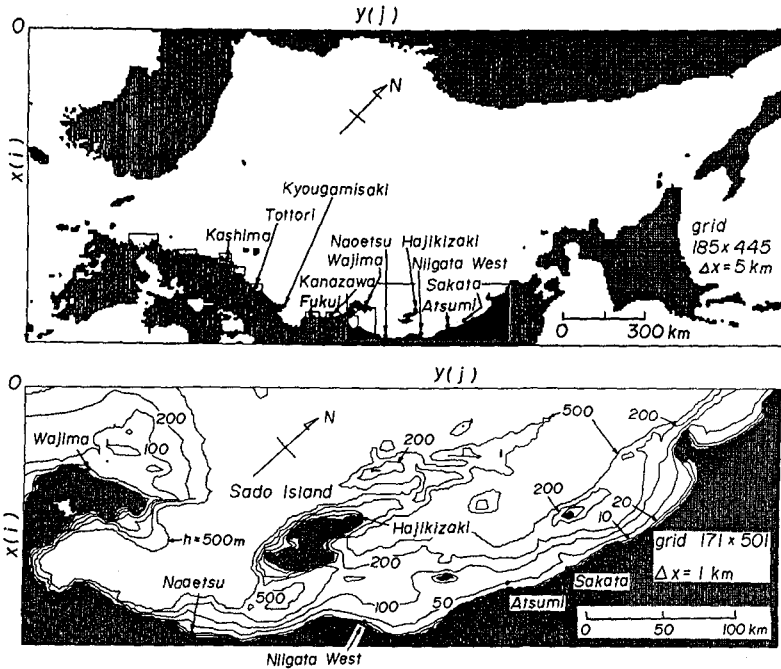


Fig.2 Medium and fine grid systems used in wave hindcast and location of hindcast points.

Wave ray is traced on the nesting grid system composed of the Japan Sea area divided into 185 by 445 with a medium grid size of 5 km and a small sea area surrounding the hindcast point with a fine grid size of 1 km. Fig. 2 shows the medium grid system covering the Japan sea and an example of the fine grid system covering the coastal area off the Hokuriku District, which are used in wave ray computation. The figures also include the locations of 11 wave hindcast points and contour plot of water depth. The numbers of frequency and direction data are 25 and 20 to 25 respectively, and the time step in wave hindcasting is 1 hour. Wind speeds and directions at wave computation points along a wave ray are estimated by applying a bilinear interpolation formula to wind data at 4 wind grid points surrounding the wave computation point. Boundary around the computational sea area is assumed to be land, where the directional spectrum is zero.

Since it is assumed to be three days after the start of computation that the influence of initial condition of calm sea vanishes, the wave hindcasting is carried out every hour for about 8 years from 4 a.m., December 29th, 1981 until 12 p.m., December 31st, 1989.

Fig. 3 is an example of refraction diagram. Directional range of wave rays reaching a hindcast point rather changes every hindcast point due to geographical situation in the vicinity of the hindcast point.

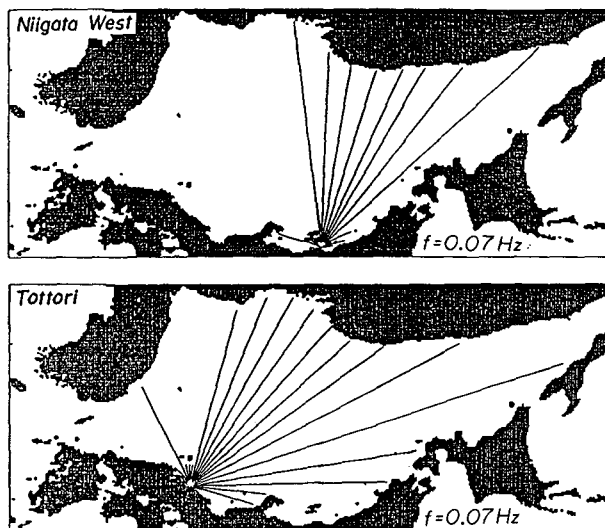


Fig. 3 Examples of refraction diagram at wave hindcast point.

3. Applicability of Long-Term Wave Hindcast System

(1) Comparison for time variations of significant waves

Spiky noises are often found in the time series of significant wave period data observed during the calm sea state. In general, data observed during the low wave condition are less reliable compared to those during the high wave condition, because of measuring and statistical errors. Thus, wave observation data to be used for comparison with hindcasted results are limited to those which satisfy the condition such as $H_{1/3\text{obs}}/1.56T_{1/3\text{obs}}^2 > 0.003$, where $H_{1/3}$ is the significant wave height, $T_{1/3}$ the significant wave period, and subscripts 'obs' and 'cal' indicate the observed and hindcasted results respectively. The threshold value of 0.003 is conveniently adopted only for excluding unfavorable observation data and does not have any physical meaning.

Fig. 4 is two examples of the 3 month comparison between hindcast and observation for the time variations of wave height, period and wave direction at Wajima and Tottori indicated in Fig. 2. Wave hindcast was carried out with both the shallow water wave model and the deep water wave model. Both models follow the time variations of

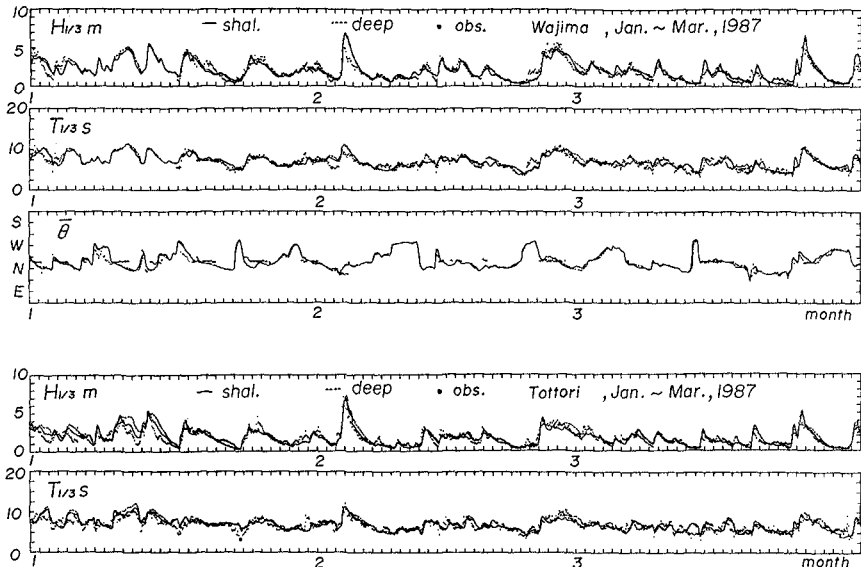


Fig. 4 Comparison between hindcast and observation for time variations of significant waves over 3 months at Wajima and Tottori.

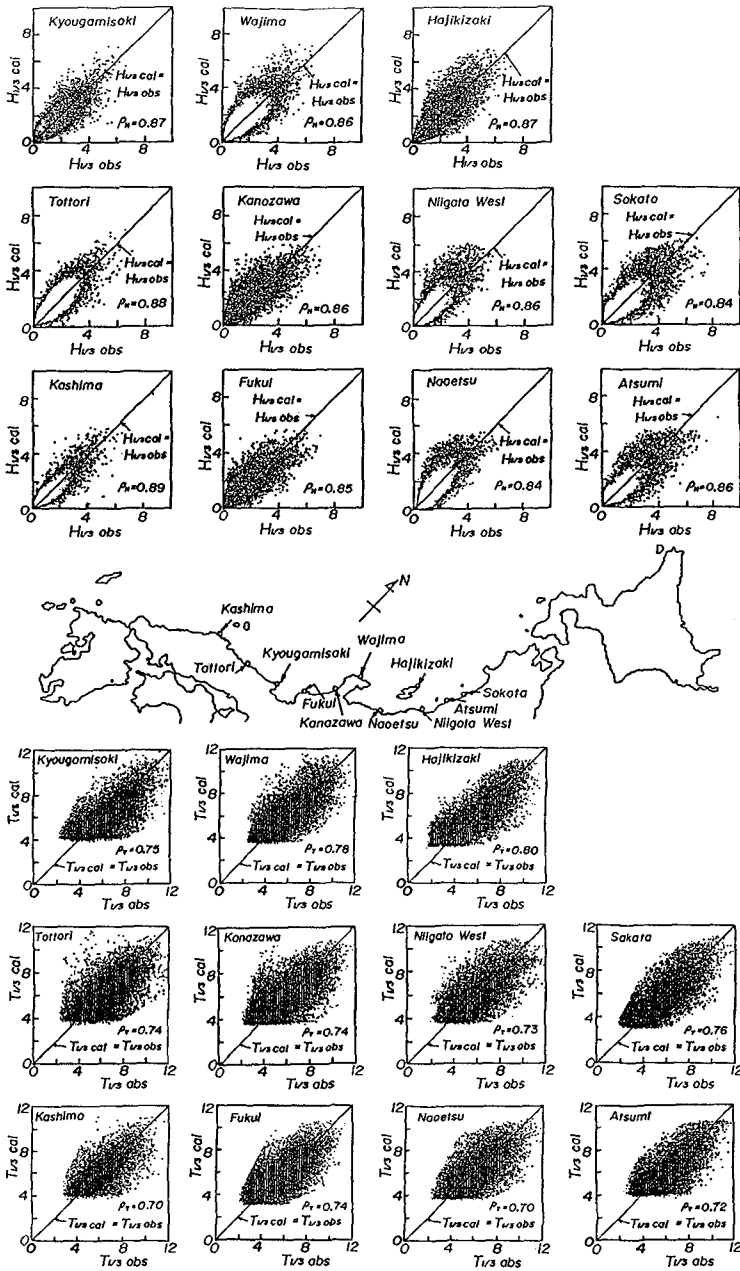


Fig. 5 Scatter diagrams between hindcast and observation for significant waves.

observed waves with acceptable accuracy, and the shallow water wave model gives better estimation than the deep water model during the high wave condition. Hereafter wave hindcast with the shallow water wave model is used for the comparison with wave observation, where no reference is made.

High reliability of the present system is also confirmed in Fig. 5 indicating the scatter diagrams of individual significant wave height and period observed every 2 or 3 hours over 8 years at 11 points along the coast of the Japan Sea. Plotted points almost symmetrically distribute around the line which means the perfect correlation between hindcast and observation, but plotted data for wave period show wider scatter than those for wave height. Accordingly, the correlation coefficient for wave height ρ_H ranges from 0.84 to 0.89, while the correlation coefficient for wave period ρ_T shows smaller value of 0.70 to 0.80 than those for wave height.

(2) Comparison for wave climate

Fig. 6 shows the error statistics on yearly-averaged wave height and period at 11 wave observation points along the coast of the Japan Sea, in which $\bar{H}_{1/3}$ and

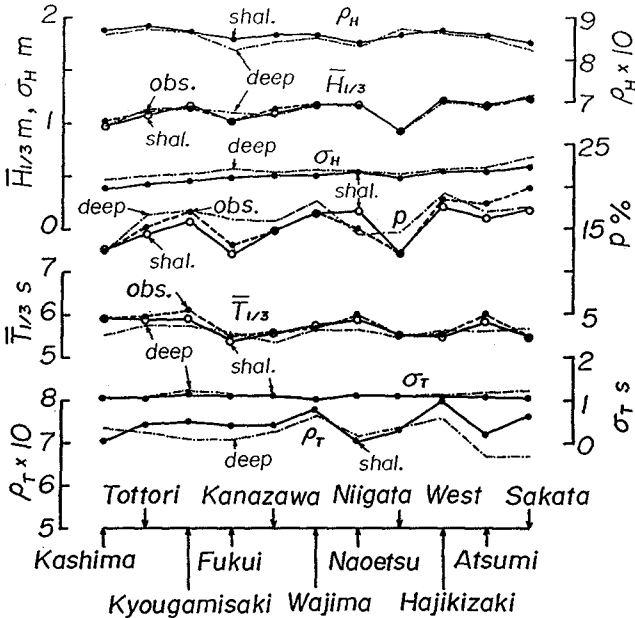


Fig. 6 Error statistics on significant waves hindcasted consecutively over 8 years at 11 points along the coast of the Japan Sea.

$\overline{T_{1/3}}$ are the yearly-averaged significant wave height and period, σ_H and σ_T the root-mean square errors of wave height and period and p is the occurrence rate of high waves exceeding wave height of 2 m. Overall agreement between hindcast and observation is found in the figure, although wave period is nearly consistently underestimated by about 0.3 s, and the shallow water wave model gives higher correlation coefficient and smaller root-mean square error for both wave height and wave period than the deep water wave model. As for the occurrence rate of high waves, the shallow water wave model has a tendency of underestimation, whereas the deep water wave model has a tendency of overestimation.

Fig. 7 is the monthly variations of mean significant wave height and period and occurrence rate of the high

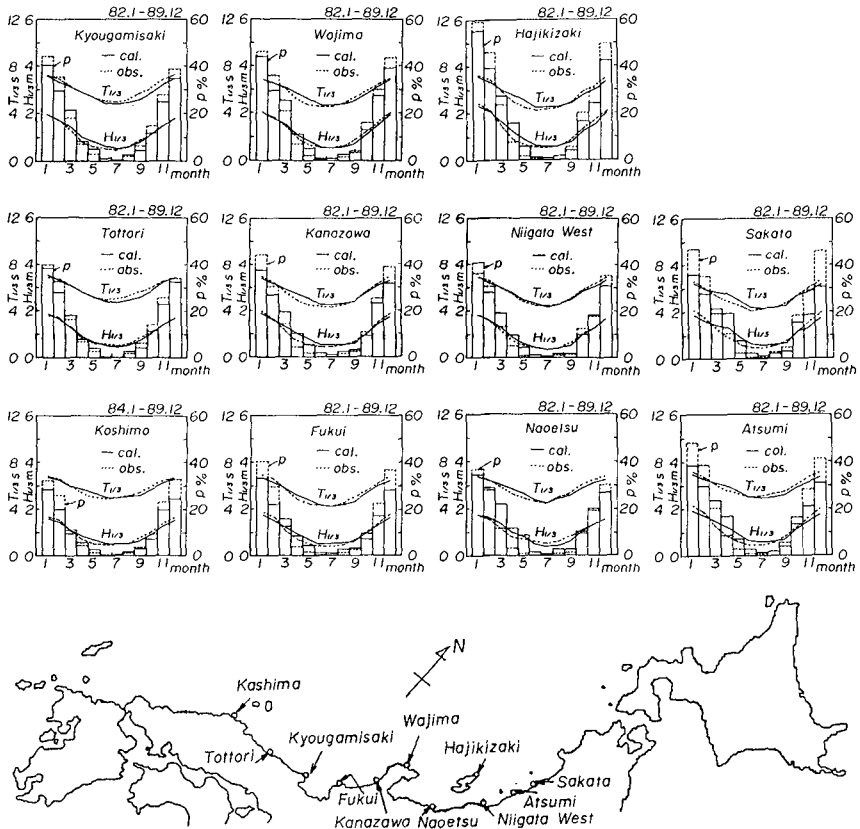


Fig. 7 Comparison of hindcast and observation for monthly variations of mean significant waves and occurrence rate of high waves.

waves at 11 points which are indices representing wave climate. The model reproduces fairly well the seasonal change of wave climate in the Japan Sea where high wave conditions occur in winter and autumn, and calm sea states continue in summer and spring. More precisely, the model tends to overestimate the wave conditions during April to September and to underestimate the one during September to December.

Fig. 8 shows the comparison between computation and observation for histograms of wave height grouped every 0.5 m and wave period grouped every 1 s. The model reproduces well overall distribution of the histograms again. But, underestimation for the occurrence rate of wave height with 0 to 0.5 m and overestimation for the occurrence rate of wave height with 0.5 to 1 m or the contrary tendency are found in the hindcast points located in the northern part of the coast of the Japan Sea such as Naoetsu and Sakata. The model also tends to overestimate the occurrence rates of wave period with 4 to 6 s and to underestimate those of the other ranges.

The above-mentioned applicability of the model is also confirmed in Fig. 9 which shows the comparison for contour plot of correlation between significant wave height and period. As the Japan Sea is almost closed, being surrounded by land boundaries, wind waves are predominant, which have high correlation between wave height and wave period. The model reproduces fairly well the feature of observed data which is described by contour lines extending in the right-upward direction.

Fig. 10 illustrates the comparison of hindcast and observation for the directionally-grouped occurrence rates of high wind speed exceeding 10 m/s and those of wave height exceeding 2 m at 5 observation points. The number of observation data of mean wave direction is much smaller than that of hindcast data used in the analysis, because of the reasons such as undeployment of wave direction measurement device and its break-down by severe sea states. The period of wind observation data used in the analysis is 8 years from 1982 to 1989 at Wajima, 2 years from 1986 to 1987 at Sakata, Hajikizaki and Fukui, and 1 year of 1986 at Niigata West.

At Hajikizaki facing open sea directly, high correlation for the directionally-grouped occurrence rates of both high winds and high waves is found and the distributions of hindcasted data agree well with those of observed data. Difference between the distributions by both shallow water wave model and deep water wave model is small, because water depth of 50 m at Hajikizaki gives almost deep water wave condition even for high waves with

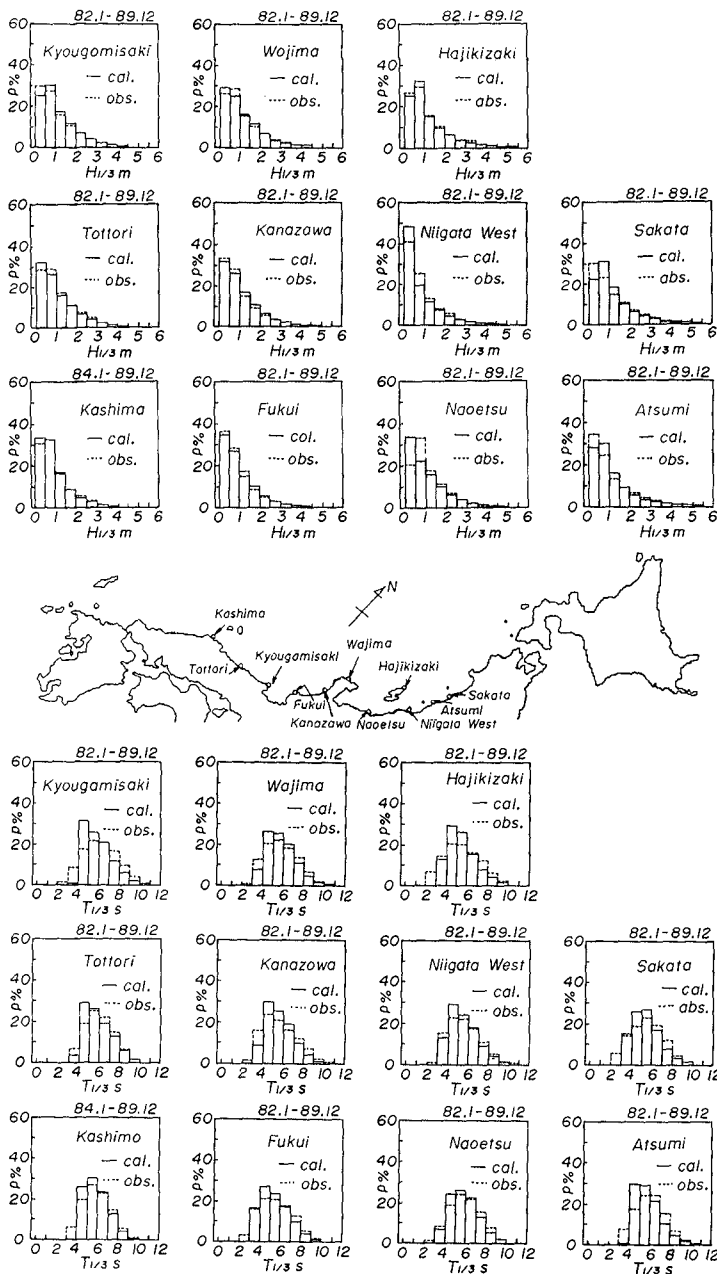


Fig. 8 Comparison of hindcast and observation for histograms of significant wave height and period.

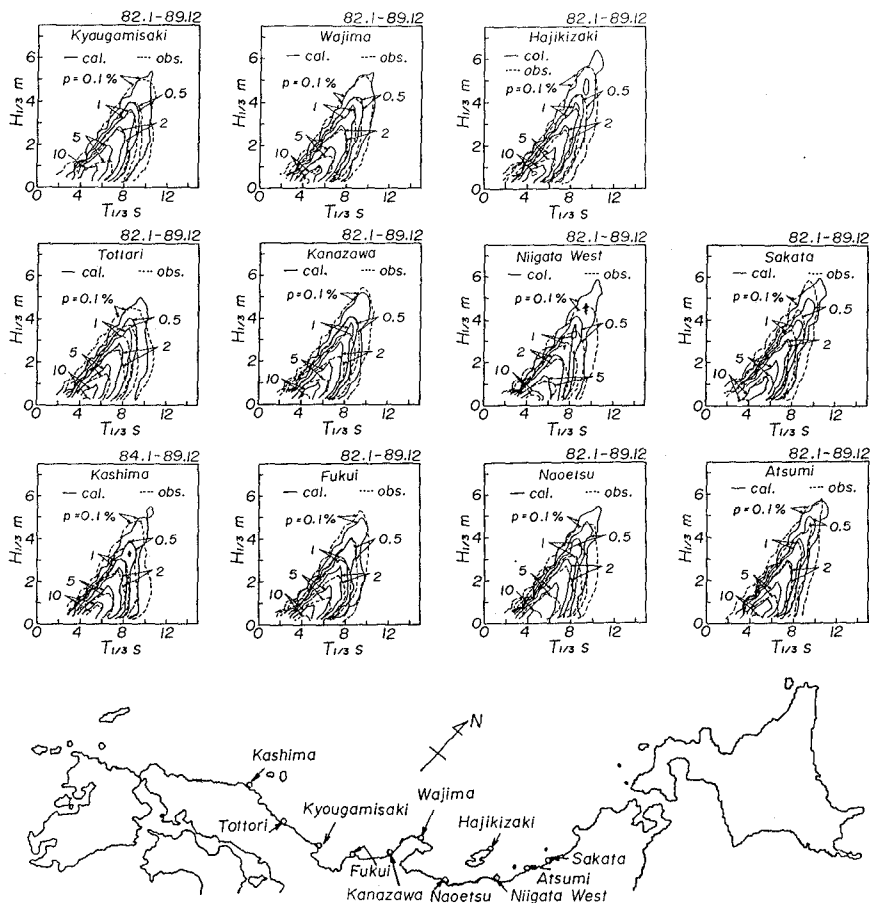


Fig. 9 Comparison of hindcast and observation for correlation diagram between wave height and wave period.

wave period shorter than about 10 s. On the other hand, predominant wave directions estimated by both shallow and deep water wave models at Wajima, where is in observation conditions similar to Hajikizaki are biased against observed wave direction clockwise by about 10 degrees, as estimated predominant wind direction is biased against observed wind direction to similar extent. Observation points at Sakata, Niigata West and Fukui are located in shallow water where water depths are less than 30 m. At Niigata West, predominant wave directions hindcasted with both models are close to the observed direction in

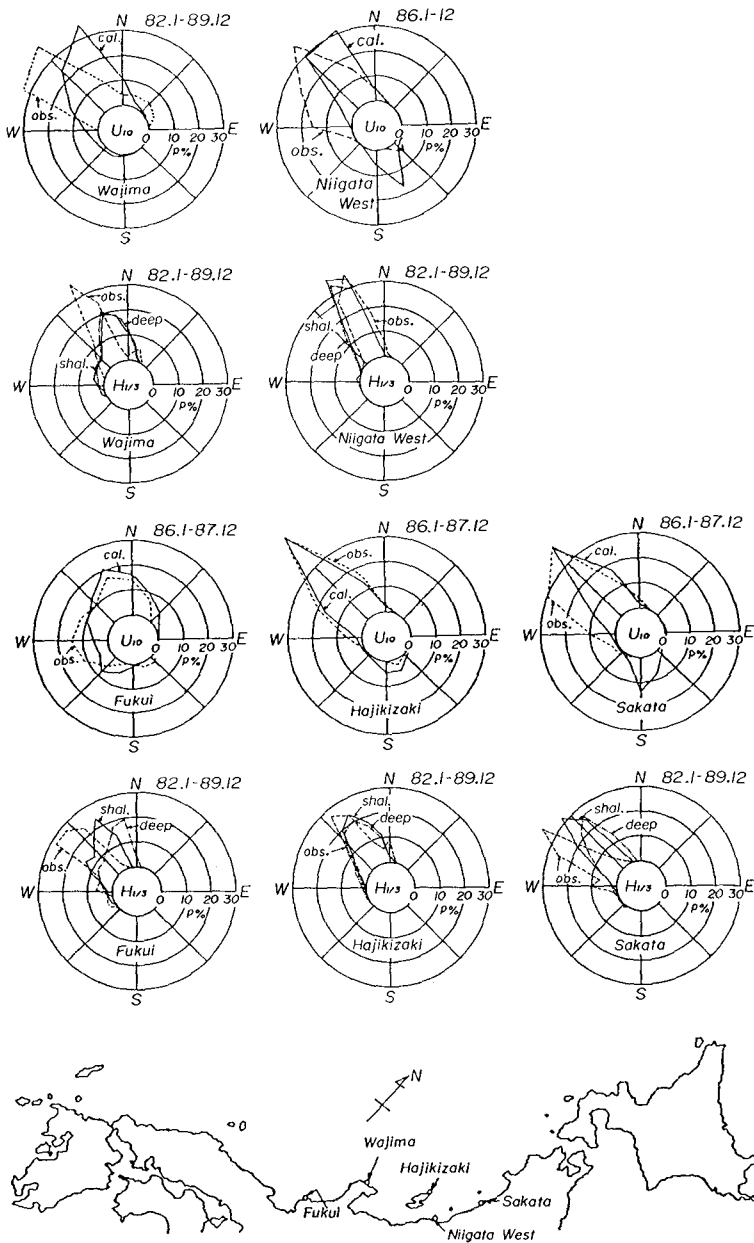


Fig. 10 Comparison of hindcast and observation for directionally-grouped occurrence rates of high winds and high waves.

spite of the difference of predominant wind direction. This suggests that sheltering effect of Sado Island is greater than refraction effect at Niigata West. At Fukui and Sakata, the shallow water wave model gives better estimation to observed predominant wave direction than the deep water wave model, but discrepancy of about 20 degrees still exists.

4. Conclusions

Applicability of the long term wave hindcast system was verified by reasonable agreement between computation and observation over 8 years at 11 wave observation points along the coast of the Japan Sea. Although the shallow water wave model requires more than three times computer processing time compared to the deep water wave model, higher reliability over the deep water wave model leads us to use the shallow water wave model for the estimation of wave climate including wave direction.

5. Acknowledgements

The authors thank the Bureaus of Harbor Construction, Ministry of Transportation and the Prefectural Offices for kindly offering the valuable wind and wave data. Thanks are also due to Mr. M. Ohfuku, Technical Officer of Civil and Ocean Engineering, Ehime University and Mr. T. Hioki, graduate student of Ocean Engineering, Ehime University for their sincere assistance during the study.

References

- Bijvoet, H.C.(1957): A new overlay for the determination of the surface wind over sea from surface weather charts, KNMI, Mededelingen en Verhandelingen, Vol. 71, pp. 1-35.
- Thornton, E.B.(1977): Rederivation of the saturation range in the frequency spectrum of wind-generated gravity waves, J. Phys. Oceanogr., Vol. 7, No. 1, pp. 137-140.
- Yamaguchi, M. et al.(1987): A shallow water wave prediction model at a single location and its applicability, Proc. JSCE, No. 381/II-7, pp. 151-160(in Japanese).
- Yamaguchi, M. et al.(1990): Estimation of wave climate along the coast of the Japan Sea based on wave hindcasting, Natural Disaster Science, 9-3, pp. 18-42(in Japanese).